



Crystal structure, Hirshfeld surface analysis and geometry optimization of 2-hydroxyimino-*N*-[1-(pyrazin-2-yl)ethylidene]propanohydrazide

Maksym O. Plutenko,^{a*} Svitlana V. Shishkina,^{b,c} Oleg V. Shishkin,^b Vadim A. Potaskalov^d and Valentina A. Kalibabchuk^e

Received 22 July 2022

Accepted 5 August 2022

Edited by L. Van Meervelt, Katholieke Universiteit Leuven, Belgium

Keywords: crystal structure; hydrazide; hydrazone; oxime; Schiff base; polynucleative ligand.

CCDC reference: 2195126

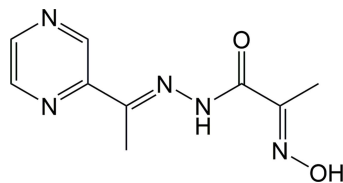
Supporting information: this article has supporting information at journals.iucr.org/e

^aDepartment of Chemistry, National Taras Shevchenko University, Volodymyrska Street 64, 01601 Kyiv, Ukraine, ^bInstitute for Single Crystals" NAS of Ukraine, 60 Nauky ave., Kharkiv, 61001, Ukraine, ^cV. N. Karazin Kharkiv National University, 4 Svobody sq., Kharkiv 61022, Ukraine, ^dDepartment of General and Inorganic Chemistry, National Technical University of Ukraine, 'Kyiv Polytechnic Institute', 37 Prospect Peremogy, 03056 Kiev, Ukraine, and ^eDepartment of Analytical, Physical and Colloid Chemistry, O. O. Bohomolets National Medical University, Shevchenko Blvd. 13, 01601 Kiev, Ukraine. *Correspondence e-mail: plutenkom@gmail.com

In the molecule of the title compound, C₉H₁₁N₅O₂, the oxime and hydrazide groups are situated in a *cis*-position in relation to the C—C bond linking the two functional groups. The CH₃C(=NOH)C(O)NH fragment deviates from planarity because of a twist between the oxime and amide groups. In the crystal, molecules are linked by O—H...O hydrogen bonds, forming zigzag chains in the [013] and [0 $\bar{1}$ 3] directions.

1. Chemical context

The combination in one molecule of two donor sets of a different nature, such as oxime and hydrazide, might be the key to creating new asymmetric polynucleative ligands suitable for the formation of polynuclear complexes. In recent decades, a number of ligands based on 2-hydroxyimino-propanehydrazide have been obtained. It was shown that such a type of ligand reveals a strong tendency for the formation of polynuclear complexes (Anwar *et al.*, 2011, 2012; Fritsky *et al.*, 2006; Jin *et al.*, 2022).



The title compound, 2-hydroxyimino-*N*-[1-(pyrazin-2-yl)ethylidene]propanohydrazide (**1**), was first described in the work of Feng and co-workers (Feng *et al.*, 2018). It acts as a ligand in three new polynuclear heterometal porous coordination polymers, which have displayed high CO₂ adsorption uptake and high adsorption selectivity of CO₂ over N₂ and CH₄. The present work is devoted to the synthesis, crystal structure, spectroscopic characterization, Hirshfeld surface analysis and quantum mechanical geometry optimization of **1**.

2. Structural commentary

The title compound, **1**, crystallizes in space group *Pca*2₁ (Fig. 1). The N—O and C—N bond lengths of the oxime group

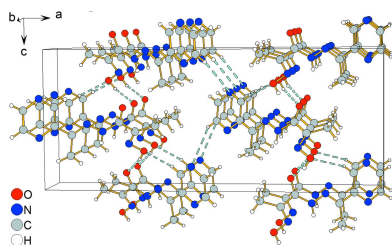


Table 1
 Hydrogen-bond geometry (Å, °).

$D-H\cdots A$	$D-H$	$H\cdots A$	$D\cdots A$	$D-H\cdots A$
$O2-H2\cdots O1^i$	0.82	1.94	2.741 (3)	167
$C2-H2A\cdots O2^{ii}$	0.93	2.35	3.243 (5)	161
$C4-H4A\cdots N2^{iii}$	0.93	2.67	3.451 (6)	142

Symmetry codes: (i) $-x + \frac{3}{2}, y + 1, z + \frac{1}{2}$; (ii) $-x + \frac{3}{2}, y - 1, z - \frac{1}{2}$; (iii) $-x + 1, -y - 1, z + \frac{1}{2}$.

are 1.382 (3) and 1.278 (4) Å, respectively, which is typical for neutral moieties of this type (Fritsky *et al.*, 1998, 2004). The N–N, N–C and C–O bond lengths of the hydrazide group [1.370 (3), 1.332 (4) and 1.229 (4) Å, respectively] are typical for 2-(hydroxyimino)propanehydrazide derivatives (Hegde *et al.*, 2017; Malinkin *et al.*, 2012; Moroz *et al.*, 2009*a,b*; Plutenko *et al.*, 2011). The oxime and the hydrazide groups are situated in a *cis*-position about the C7–C8 bond, which is also typical for 2-(hydroxyimino)propanehydrazide derivatives. Such a conformation is stabilized additionally by an H4···N5 attractive interaction (2.33 Å). Despite the distance being shorter than the sum of the van der Waals radii (2.67 Å; Zefirov, 1997) the interaction cannot be classified as an intramolecular hydrogen bond because of the acute N4–H···N5 angle (101°).

The $CH_3C(=NOH)C(O)NH$ fragment deviates from planarity (r.m.s. deviation of 0.362 Å) because of a twist between the oxime and the amide groups about the C7–C8 bond. The maximum deviations are 0.8763 (9) and 0.3355 (18) Å, respectively, for hydrogen (H9C) and non-hydrogen (O1) atoms. The O1–C7–C8–N5 torsion angle is 165.1 (3)°, significantly less than the average value in 2-(hydroxyimino)propanehydrazide derivatives published previously [172.1 (4)°]. Thus, such a twist distortion of the molecule seems to be a result of the crystal packing.

3. Supramolecular features

In the crystal, molecules are linked by $O2-H2\cdots O1^i$ and $C2-H2A\cdots O2^{ii}$ intermolecular hydrogen bonds [symmetry codes: (i) $-x + \frac{3}{2}, y + 1, z + \frac{1}{2}$; (ii) $-x + \frac{3}{2}, y - 1, z - \frac{1}{2}$], forming

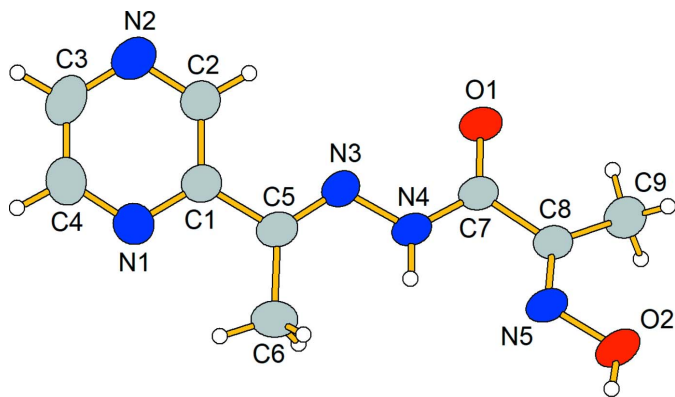


Figure 1
 The molecular structure of the title compound **1** with displacement ellipsoids shown at the 50% probability level.

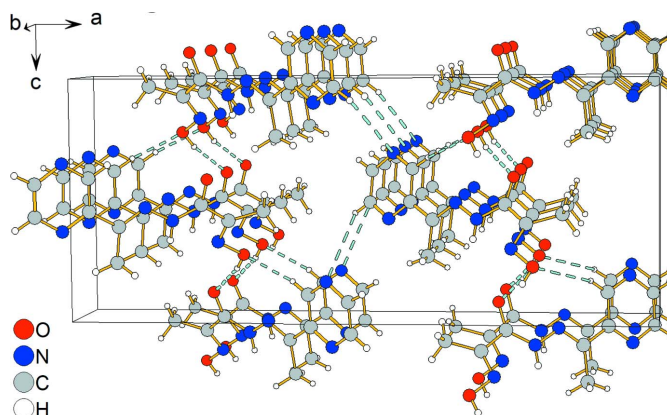


Figure 2
 Crystal packing of the title compound **1**. Hydrogen bonds are indicated by dashed lines.

zigzag chains in the [013] and $[0\bar{1}3]$ crystallographic directions (Fig. 2). These chains alternate in the [100] direction and are linked by $C4-H4A\cdots N2^{iii}$ intermolecular hydrogen bonds [symmetry code: (iii) $-x + 1, -y - 1, z + \frac{1}{2}$]. Details of the hydrogen-bond geometry are given in Table 1.

4. Hirshfeld surface analysis

The Hirshfeld surface analysis (Spackman & Jayatilaka, 2009) and the associated two-dimensional fingerprint plots (McKinnon *et al.*, 2007) were performed with *Crystal-*

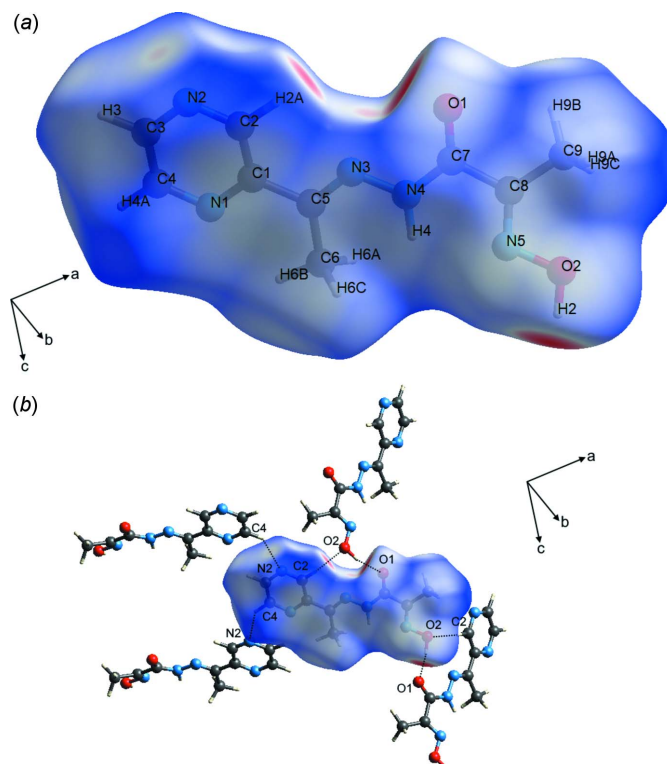


Figure 3
 The Hirshfeld surface of the title molecule **1** mapped over d_{norm} , showing the close contacts.

Explorer17 (Turner *et al.*, 2017). The Hirshfeld surfaces of the complex anions are colour-mapped with the normalized contact distance (d_{norm}) from red (distances shorter than the sum of the van der Waals radii) through white to blue (distances longer than the sum of the van der Waals radii). The Hirshfeld surface of the title compound mapped over d_{norm} , in the colour range -0.6441 to 1.3084 a.u. is shown in Fig. 3. According to the Hirshfeld surface, $\text{O2}\cdots\text{H2}\cdots\text{O1}$ and $\text{C4}\cdots\text{H4A}\cdots\text{N2}$ are the most noticeable intermolecular interactions. In addition, a $\text{C2}\cdots\text{H2A}\cdots\text{O2}$ weak intermolecular interaction is observed.

A fingerprint plot delineated into specific interatomic contacts contains information related to specific intermolecular interactions. The blue colour refers to the frequency of occurrence of the (d_i , d_e) pair with the full fingerprint plot outlined in grey. Fig. 4 shows the two-dimensional fingerprint plots of the sum of the contacts contributing to the Hirshfeld surface represented in normal mode. The most significant contribution to the Hirshfeld surface is from $\text{H}\cdots\text{H}$ (41.9%) contacts. In addition, $\text{N}\cdots\text{H}/\text{H}\cdots\text{N}$ (20.5%) and $\text{O}\cdots\text{H}/\text{H}\cdots\text{O}$ (15.4%) are highly significant contributions to the total Hirshfeld surface. The $\text{O}\cdots\text{H}/\text{H}\cdots\text{O}$ fingerprint plot (Fig. 4d) reveals two sharp spikes along $1.9 \text{ \AA} < d_i + d_e < 2.4 \text{ \AA}$, which are associated with the $\text{O2}\cdots\text{H2}\cdots\text{O1}$ hydrogen bond.

5. Geometry optimization

The DFT quantum-chemical calculations were performed at the B3LYP/6-311 G(d,p) level (Becke, 1993) as implemented in *PSI4* software package (Parrish *et al.*, 2017). The GFN2-

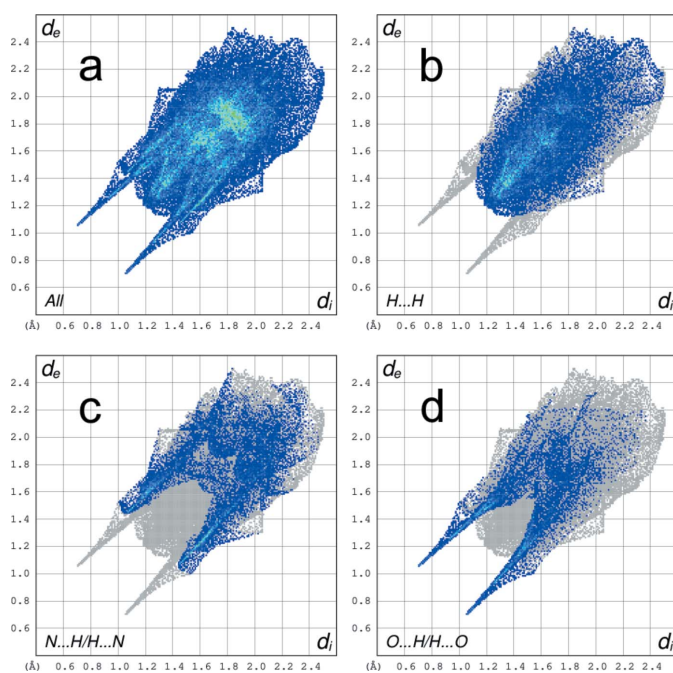


Figure 4
A view of the two-dimensional fingerprint plots for the title compound **1** showing (a) all interactions, and delineated into (b) $\text{H}\cdots\text{H}$ (41.9%), (c) $\text{N}\cdots\text{H}/\text{H}\cdots\text{N}$ (20.5%) and (d) $\text{O}\cdots\text{H}/\text{H}\cdots\text{O}$ (15.4%) contacts.

Table 2
Comparison of selected geometric data (\AA , $^\circ$) from calculated and X-ray data.

	X-ray	DFT	GFN2-xTB
Oxime moiety			
$\text{C8}=\text{N5}$	1.278 (4)	1.285	1.273
$\text{N5}-\text{O2}$	1.382 (3)	1.394	1.389
$\text{C8}-\text{N5}-\text{O2}$	111.4 (2)	112.1	116.0
Hydrazide moiety			
$\text{C7}=\text{O1}$	1.229 (4)	1.218	1.208
$\text{C7}-\text{N4}$	1.332 (4)	1.382	1.368
$\text{N3}-\text{N4}$	1.370 (3)	1.351	1.336
$\text{O1}-\text{C7}-\text{N4}$	124.1 (3)	124.6	124.7
Other			
$\text{C5}=\text{N3}$	1.278 (4)	1.292	1.279
$\text{O1}-\text{C7}-\text{C8}-\text{N5}$	165.1 (3)	179.9	179.0

xTB (Bannwarth *et al.*, 2019) calculations were applied with *xtb 6.4* package (Grimme, 2019). The structure optimization of the title compound was performed starting from the X-ray geometry and the resulting geometric values were compared with experimental values (Table 2, Fig. 5). The r.m.s. deviations are 0.380 and 0.362 \AA for DFT and GFN2-xTB, respectively.

The calculated geometric parameters are in good agreement with experimental values. It is important to note that the accuracy of the semi-empirical GFN2-xTB method is close to that of the DFT calculations, even though GFN2-xTB calculations are significantly computationally 'cheaper' ($\sim 2 \cdot 10^3$ times faster for the calculations described here).

The most significant difference between the calculated and X-ray geometries is the absence of a twist deformation between the oxime and the amide groups in the case of QM calculated geometries. This might be additional evidence that the twist distortion of the molecule is due to effects of the crystal packing. The largest differences between the X-ray and calculated bond lengths are observed for the hydrazide moiety: $\text{N3}-\text{N4}$ is slightly longer (0.019 and 0.034 \AA for DFT and GFN2-xTB, respectively) and $\text{C7}-\text{N4}$ is shorter (0.050 and 0.036 \AA for DFT and GFN2-xTB, respectively) than calculated. Such calculation errors are probably typical for

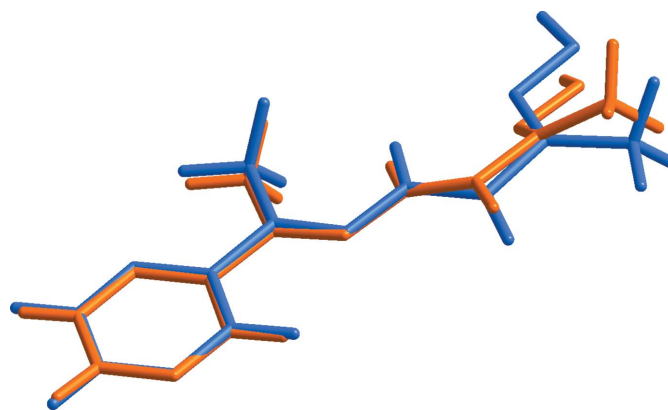


Figure 5
Overlay between the molecule obtained from experimental (orange) and DFT optimization (blue).

hydrazide derivatives at this level of theory (Anitha *et al.*, 2019; Malla *et al.*, 2022). The HOMO–LUMO gap calculated by DFT method is 0.159 a.u. and the frontier molecular orbital energies, E_{HOMO} and E_{LUMO} are -0.23063 and -0.07178 a.u., respectively.

6. Database survey

A search in the Cambridge Structural Database (CSD version 5.43, update of March 2022; Groom *et al.*, 2016) resulted in seven hits for 2-(hydroxyimino)propanehydrazide derivatives: CUDBEJ, DUDHOA, OBUXIU, PUVPED, PUVPED01, WARCEZ and WARCID (Hegde *et al.*, 2017; Malinkin *et al.*, 2012; Moroz *et al.*, 2009*a,b*; Plutenko *et al.*, 2011). Most of them deviate slightly from planarity: r.m.s. deviations are in the range 0.247–0.390 Å with maximum deviations of non-hydrogen atoms from the best plane in the range 0.098–0.340 Å. At the same time PUVPED and PUVPED01 are not planar, mainly because of a twist of the dicarbonylhydrazine group [the C–N–N–C torsion angle is 96.54 (15)°].

157 hits relate to organometallic substances based on 2-(hydroxyimino)propanehydrazide derivatives. Most of them are polynuclear 3*d* and 4*f* metal complexes (discrete molecules and MOFs). The maximum number of metal centres per molecule for the discrete complexes of this type is 12 (Anwar *et al.*, 2011, 2012; Moroz *et al.*, 2012).

7. Synthesis and crystallization

The title compound was prepared according to a slightly modified procedure (Feng *et al.*, 2018). A solution of 2-(hydroxyimino)propanehydrazide (0.702 g, 5 mmol) in methanol (50 ml) was treated with 2-acetylpyrazine (0.732 g, 5 mmol) and the mixture was heated under reflux for 1.5 h. After that, the solvent was evaporated under vacuum and the product was recrystallized from methanol. Yield 1.141 g (86%). ^1H NMR, 400.13 MHz, (DMSO- d_6): 11.97 (*s*, 1H, OH), 10.21 (*s*, 1H, NH), 9.31 (*s*, 1H, pyrazine-3), 8.56 (*s*, 1H, pyrazine-5), 8.55 (*s*, 1H, pyrazine-6), 2.37 (*s*, 3H, hydrazonic CH₃), 2.02 (*s*, 3H, CH₃). IR (KBr, cm⁻¹): 1658 (CO amid I), 1034 (NO oxime). Analysis calculated for C₉H₁₁N₅O₂: C 48.86, H 5.01, N 31.66%; found: C 48.49, H 5.22, N 31.42%.

8. Refinement

Crystal data, data collection and structure refinement details are summarized in Table 3. All the hydrogen atoms were positioned geometrically (N–H = 0.85, C–H = 0.93–0.96 Å) and refined using a riding model with $U_{\text{iso}} = nU_{\text{eq}}$ of the carrier atom ($n = 1.5$ for methyl groups and $n = 1.2$ for other hydrogen atoms).

Funding information

This work was supported by the Ministry of Education and Science of Ukraine: Grant of the Ministry of Education and Science of Ukraine for perspective development of the

Table 3
Experimental details.

Crystal data	
Chemical formula	C ₉ H ₁₁ N ₅ O ₂
M_r	221.23
Crystal system, space group	Orthorhombic, <i>Pca</i> 2 ₁
Temperature (K)	293
a, b, c (Å)	24.367 (2), 4.3979 (5), 10.1424 (9)
V (Å ³)	1086.89 (18)
Z	4
Radiation type	Mo $K\alpha$
μ (mm ⁻¹)	0.10
Crystal size (mm)	0.8 × 0.4 × 0.1
Data collection	
Diffractometer	Xcallibur3
Absorption correction	Multi-scan (<i>CrysAlis PRO</i> ; Rigaku OD, 2019)
$T_{\text{min}}, T_{\text{max}}$	0.646, 1.000
No. of measured, independent and observed [$I > 2\sigma(I)$] reflections	2381, 1540, 1254
R_{int}	0.023
($\sin \theta/\lambda$) _{max} (Å ⁻¹)	0.595
Refinement	
$R[F^2 > 2\sigma(F^2)], wR(F^2), S$	0.037, 0.088, 1.01
No. of reflections	1540
No. of parameters	148
No. of restraints	1
H-atom treatment	H-atom parameters constrained
$\Delta\rho_{\text{max}}, \Delta\rho_{\text{min}}$ (e Å ⁻³)	0.11, -0.13
Absolute structure	Flack x determined using 351 quotients $[(I^+) - (I^-)] / [(I^+) + (I^-)]$ (Parsons <i>et al.</i> , 2013)
Absolute structure parameter	-1.7 (10)

Computer programs: *CrysAlis PRO* (Rigaku OD, 2019), *SHELXT* (Sheldrick, 2015*a*), *SHELXL2016/6* (Sheldrick, 2015*b*), *DIAMOND* (Brandenburg, 2009) and *OLEX2* (Dolomanov *et al.*, 2009).

scientific direction ‘Mathematical sciences and natural sciences’ at Taras Shevchenko National University of Kyiv.

References

- Anitha, A. G., Arunagiri, C. & Subashini, A. (2019). *Acta Cryst.* **E75**, 109–114.
- Anwar, M. U., Dawe, L. N., Alam, M. S. & Thompson, L. K. (2012). *Inorg. Chem.* **51**, 11241–11250.
- Anwar, M. U., Dawe, L. N. & Thompson, L. K. (2011). *Dalton Trans.* **40**, 8079–8082.
- Bannwarth, C., Ehlert, S. & Grimme, S. (2019). *J. Chem. Theory Comput.* **15**, 1652–1671.
- Becke, A. D. (1993). *J. Chem. Phys.* **98**, 5648–5652.
- Brandenburg, K. (2009). *DIAMOND*. Crystal Impact GbR, Bonn, Germany.
- Dolomanov, O. V., Bourhis, L. J., Gildea, R. J., Howard, J. A. K. & Puschmann, H. (2009). *J. Appl. Cryst.* **42**, 339–341.
- Feng, D.-D., Dong, H.-M., Liu, Z.-Y., Zhao, X.-J. & Yang, E.-C. (2018). *Dalton Trans.* **47**, 15344–15352.
- Fritsky, I. O., Kozłowski, H., Kanderl, O. M., Haukka, M., Świątek-Kozłowska, J., Gumienna-Kontecka, E. & Meyer, F. (2006). *Chem. Commun.* pp. 4125–4127.
- Fritsky, I. O., Kozłowski, H., Sadler, P. J., Yefetova, O. P., Świątek-Kozłowska, J., Kalibabchuk, V. A. & Głowiak, T. (1998). *J. Chem. Soc. Dalton Trans.* pp. 3269–3274.
- Fritsky, I. O., Świątek-Kozłowska, J., Dobosz, A., Sliva, T. Y. & Dudarenko, N. M. (2004). *Inorg. Chim. Acta*, **357**, 3746–3752.

- Grimme, S. (2019). *xtb 6.4*. Mulliken Center for Theoretical Chemistry, University of Bonn, Germany.
- Groom, C. R., Bruno, I. J., Lightfoot, M. P. & Ward, S. C. (2016). *Acta Cryst.* **B72**, 171–179.
- Hegde, D., Naik, G. N., Vadavi, R. S., Barretto, D. A. & Gudasi, K. B. (2017). *Inorg. Chim. Acta*, **461**, 301–315.
- Jin, Y.-S., Wang, X., Zhang, N., Liu, C.-M. & Kou, H.-Z. (2022). *Cryst. Growth Des.* **22**, 1263–1269.
- Malinkin, S. O., Penkova, L., Moroz, Y. S., Haukka, M., Maciag, A., Gumienna-Kontecka, E., Pavlenko, V. A., Pavlova, S., Nordlander, E. & Fritsky, I. O. (2012). *Eur. J. Inorg. Chem.* pp. 1639–1649.
- Malla, M. A., Bansal, R., Butcher, R. J. & Gupta, S. K. (2022). *Acta Cryst.* **E78**, 1–7.
- McKinnon, J. J., Jayatilaka, D. & Spackman, M. A. (2007). *Chem. Commun.* pp. 3814–3816.
- Moroz, Y. S., Demeshko, S., Haukka, M., Mokhir, A., Mitra, U., Stocker, M., Müller, P., Meyer, F. & Fritsky, I. O. (2012). *Inorg. Chem.* **51**, 7445–7447.
- Moroz, Y. S., Kalibabchuk, V. A., Gumienna-Kontecka, E., Skopenko, V. V. & Pavlova, S. V. (2009a). *Acta Cryst.* **E65**, o2413.
- Moroz, Y. S., Konovalova, I. S., Iskenderov, T. S., Pavlova, S. V. & Shishkin, O. V. (2009b). *Acta Cryst.* **E65**, o2242.
- Parrish, R. M., Burns, L. A., Smith, D. G. A., Simmonett, A. C., DePrince, A. E. III, Hohenstein, E. G., Bozkaya, U., Sokolov, A. Yu., Di Remigio, R., Richard, R. M., Gonthier, J. F., James, A. M., McAlexander, H. R., Kumar, A., Saitow, M., Wang, X., Pritchard, B. P., Verma, P., Schaefer, H. F. III, Patkowski, K., King, R. A., Valeev, E. F., Evangelista, F. A., Turney, J. M., Crawford, T. D. & Sherrill, C. D. (2017). *J. Chem. Theory Comput.* **13**, 3185–3197.
- Parsons, S., Flack, H. D. & Wagner, T. (2013). *Acta Cryst.* **B69**, 249–259.
- Plutenko, M. O., Lampeka, R. D., Moroz, Y. S., Haukka, M. & Pavlova, S. V. (2011). *Acta Cryst.* **E67**, o3282–o3283.
- Rigaku OD (2019). *CrysAlis PRO*. Rigaku Oxford Diffraction Ltd, Tokyo, Japan.
- Sheldrick, G. M. (2015a). *Acta Cryst.* **A71**, 3–8.
- Sheldrick, G. M. (2015b). *Acta Cryst.* **C71**, 3–8.
- Spackman, M. A. & Jayatilaka, D. (2009). *CrystEngComm*, **11**, 19–32.
- Turner, M. J., McKinnon, J. J., Wolff, S. K., Grimwood, D. J., Spackman, P. R., Jayatilaka, D. & Spackman, M. A. (2017). *CrystalExplorer17*. University of Western Australia. <http://hirshfeldsurface.net>
- Zefirov, Yu. V. (1997). *Kristallografiya*, **42**, 936–958.

supporting information

Acta Cryst. (2022). E78, 900-904 [https://doi.org/10.1107/S2056989022007927]

Crystal structure, Hirshfeld surface analysis and geometry optimization of 2-hydroxyimino-*N*-[1-(pyrazin-2-yl)ethylidene]propanohydrazide

Maksym O. Plutenko, Svitlana V. Shishkina, Oleg V. Shishkin, Vadim A. Potaskalov and Valentina A. Kalibabchuk

Computing details

Data collection: *CrysAlis PRO* (Rigaku OD, 2019); cell refinement: *CrysAlis PRO* (Rigaku OD, 2019); data reduction: *CrysAlis PRO* (Rigaku OD, 2019); program(s) used to solve structure: *SHELXT* (Sheldrick, 2015a); program(s) used to refine structure: *SHELXL2016/6* (Sheldrick, 2015b); molecular graphics: *DIAMOND* (Brandenburg, 2009); software used to prepare material for publication: *OLEX2* (Dolomanov *et al.*, 2009).

2-hydroxyimino-*N*-[1-(pyrazin-2-yl)ethylidene]propanohydrazide

Crystal data

$C_9H_{11}N_5O_2$

$M_r = 221.23$

Orthorhombic, *Pca*2₁

$a = 24.367$ (2) Å

$b = 4.3979$ (5) Å

$c = 10.1424$ (9) Å

$V = 1086.89$ (18) Å³

$Z = 4$

$F(000) = 464$

$D_x = 1.352$ Mg m⁻³

Mo $K\alpha$ radiation, $\lambda = 0.71073$ Å

Cell parameters from 1825 reflections

$\theta = 2.4$ – 25.3°

$\mu = 0.10$ mm⁻¹

$T = 293$ K

Plate, colourless

$0.8 \times 0.4 \times 0.1$ mm

Data collection

Xcalibur3

diffractometer

area detector scans

Absorption correction: multi-scan
(*CrysAlisPro*; Rigaku OD, 2019)

$T_{\min} = 0.646$, $T_{\max} = 1.000$

2381 measured reflections

1540 independent reflections

1254 reflections with $I > 2\sigma(I)$

$R_{\text{int}} = 0.023$

$\theta_{\max} = 25.0^\circ$, $\theta_{\min} = 3.3^\circ$

$h = -13$ → 28

$k = -5$ → 4

$l = -12$ → 10

Refinement

Refinement on F^2

Least-squares matrix: full

$R[F^2 > 2\sigma(F^2)] = 0.037$

$wR(F^2) = 0.088$

$S = 1.01$

1540 reflections

148 parameters

1 restraint

Hydrogen site location: mixed

H-atom parameters constrained

$w = 1/[\sigma^2(F_o^2) + (0.0439P)^2]$

where $P = (F_o^2 + 2F_c^2)/3$

$(\Delta/\sigma)_{\max} = 0.001$

$\Delta\rho_{\max} = 0.11$ e Å⁻³

$\Delta\rho_{\min} = -0.13$ e Å⁻³

Absolute structure: Flack x determined using

351 quotients $[(F^-)-(I)]/[(F^+)+(I)]$ (Parsons *et al.*, 2013)

Absolute structure parameter: -1.7 (10)

Special details

Geometry. All esds (except the esd in the dihedral angle between two l.s. planes) are estimated using the full covariance matrix. The cell esds are taken into account individually in the estimation of esds in distances, angles and torsion angles; correlations between esds in cell parameters are only used when they are defined by crystal symmetry. An approximate (isotropic) treatment of cell esds is used for estimating esds involving l.s. planes.

Fractional atomic coordinates and isotropic or equivalent isotropic displacement parameters (\AA^2)

	<i>x</i>	<i>y</i>	<i>z</i>	$U_{\text{iso}}^*/U_{\text{eq}}$
O1	0.76287 (9)	0.3026 (5)	0.3893 (2)	0.0552 (6)
N1	0.54406 (13)	-0.2364 (8)	0.5790 (3)	0.0652 (9)
C1	0.58360 (13)	-0.1186 (7)	0.5054 (3)	0.0481 (9)
O2	0.80114 (8)	0.9769 (6)	0.7178 (3)	0.0571 (6)
H2	0.785835	1.067394	0.778171	0.086*
C2	0.58576 (16)	-0.1796 (10)	0.3721 (4)	0.0696 (12)
H2A	0.613875	-0.093141	0.322655	0.084*
N2	0.54979 (15)	-0.3547 (9)	0.3114 (3)	0.0802 (11)
N3	0.66429 (11)	0.1682 (6)	0.4996 (3)	0.0446 (6)
C3	0.51042 (17)	-0.4693 (10)	0.3865 (5)	0.0718 (13)
H3	0.483903	-0.592846	0.348009	0.086*
N4	0.70225 (10)	0.3562 (6)	0.5568 (3)	0.0457 (7)
H4	0.696761	0.411873	0.635489	0.055*
C4	0.50756 (17)	-0.4124 (11)	0.5171 (4)	0.0766 (13)
H4A	0.479179	-0.498671	0.565696	0.092*
N5	0.76423 (10)	0.7824 (5)	0.6578 (3)	0.0447 (7)
C5	0.62427 (13)	0.0788 (7)	0.5713 (3)	0.0467 (8)
C6	0.61725 (16)	0.1548 (10)	0.7154 (4)	0.0674 (10)
H6A	0.648915	0.087367	0.763582	0.101*
H6B	0.585142	0.054609	0.748914	0.101*
H6C	0.613240	0.370690	0.725479	0.101*
C7	0.74946 (14)	0.4146 (6)	0.4956 (3)	0.0406 (7)
C8	0.78699 (12)	0.6303 (7)	0.5654 (3)	0.0421 (7)
C9	0.84549 (13)	0.6475 (9)	0.5264 (4)	0.0657 (11)
H9A	0.853496	0.847820	0.494094	0.099*
H9B	0.852677	0.501055	0.458348	0.099*
H9C	0.868223	0.604687	0.601444	0.099*

Atomic displacement parameters (\AA^2)

	U^{11}	U^{22}	U^{33}	U^{12}	U^{13}	U^{23}
O1	0.0616 (13)	0.0633 (14)	0.0408 (14)	-0.0086 (12)	0.0065 (12)	-0.0188 (13)
N1	0.0593 (18)	0.086 (2)	0.0508 (18)	-0.0195 (17)	-0.0002 (17)	0.0000 (18)
C1	0.0450 (18)	0.0568 (19)	0.043 (2)	-0.0026 (16)	-0.0017 (17)	-0.0026 (18)
O2	0.0580 (13)	0.0618 (14)	0.0516 (14)	-0.0040 (12)	-0.0033 (13)	-0.0277 (12)
C2	0.065 (2)	0.094 (3)	0.050 (3)	-0.031 (2)	0.004 (2)	-0.011 (2)
N2	0.077 (2)	0.107 (3)	0.056 (2)	-0.033 (2)	-0.003 (2)	-0.016 (2)
N3	0.0455 (14)	0.0463 (14)	0.0422 (14)	-0.0036 (13)	-0.0015 (14)	-0.0097 (13)
C3	0.061 (2)	0.084 (3)	0.071 (3)	-0.022 (2)	-0.017 (2)	-0.002 (3)

N4	0.0499 (15)	0.0495 (15)	0.0377 (14)	-0.0044 (13)	0.0022 (15)	-0.0159 (13)
C4	0.063 (2)	0.103 (3)	0.064 (3)	-0.032 (2)	-0.006 (2)	0.011 (3)
N5	0.0538 (17)	0.0427 (13)	0.0375 (16)	0.0001 (13)	-0.0038 (14)	-0.0112 (13)
C5	0.0482 (18)	0.0527 (18)	0.0392 (18)	0.0012 (16)	-0.0016 (18)	-0.0059 (16)
C6	0.069 (2)	0.091 (3)	0.042 (2)	-0.012 (2)	0.005 (2)	-0.011 (2)
C7	0.0492 (17)	0.0382 (15)	0.0342 (19)	0.0017 (14)	0.0011 (16)	-0.0074 (16)
C8	0.0481 (16)	0.0432 (15)	0.0350 (17)	-0.0003 (14)	0.0021 (16)	-0.0053 (16)
C9	0.0555 (19)	0.080 (2)	0.062 (3)	-0.0123 (19)	0.014 (2)	-0.030 (2)

Geometric parameters (Å, °)

O1—C7	1.229 (4)	N4—H4	0.8452
N1—C1	1.325 (4)	N4—C7	1.332 (4)
N1—C4	1.336 (5)	C4—H4A	0.9300
C1—C2	1.379 (5)	N5—C8	1.278 (4)
C1—C5	1.477 (4)	C5—C6	1.509 (5)
O2—H2	0.8200	C6—H6A	0.9600
O2—N5	1.382 (3)	C6—H6B	0.9600
C2—H2A	0.9300	C6—H6C	0.9600
C2—N2	1.319 (5)	C7—C8	1.496 (4)
N2—C3	1.325 (5)	C8—C9	1.482 (5)
N3—N4	1.370 (3)	C9—H9A	0.9600
N3—C5	1.279 (4)	C9—H9B	0.9600
C3—H3	0.9300	C9—H9C	0.9600
C3—C4	1.350 (6)		
C1—N1—C4	116.5 (3)	N3—C5—C1	115.8 (3)
N1—C1—C2	120.3 (3)	N3—C5—C6	124.7 (3)
N1—C1—C5	117.6 (3)	C5—C6—H6A	109.5
C2—C1—C5	122.2 (3)	C5—C6—H6B	109.5
N5—O2—H2	109.5	C5—C6—H6C	109.5
C1—C2—H2A	118.5	H6A—C6—H6B	109.5
N2—C2—C1	123.1 (4)	H6A—C6—H6C	109.5
N2—C2—H2A	118.5	H6B—C6—H6C	109.5
C2—N2—C3	115.8 (4)	O1—C7—N4	124.1 (3)
C5—N3—N4	117.4 (3)	O1—C7—C8	120.5 (3)
N2—C3—H3	119.0	N4—C7—C8	115.4 (3)
N2—C3—C4	122.1 (4)	N5—C8—C7	114.4 (3)
C4—C3—H3	119.0	N5—C8—C9	125.9 (3)
N3—N4—H4	117.9	C9—C8—C7	119.6 (3)
C7—N4—N3	120.1 (3)	C8—C9—H9A	109.5
C7—N4—H4	121.4	C8—C9—H9B	109.5
N1—C4—C3	122.3 (4)	C8—C9—H9C	109.5
N1—C4—H4A	118.9	H9A—C9—H9B	109.5
C3—C4—H4A	118.9	H9A—C9—H9C	109.5
C8—N5—O2	111.4 (2)	H9B—C9—H9C	109.5
C1—C5—C6	119.5 (3)		

O1—C7—C8—N5	165.1 (3)	N2—C3—C4—N1	0.2 (8)
O1—C7—C8—C9	-16.1 (5)	N3—N4—C7—O1	-2.1 (5)
N1—C1—C2—N2	-0.3 (7)	N3—N4—C7—C8	178.2 (2)
N1—C1—C5—N3	174.5 (3)	N4—N3—C5—C1	178.8 (2)
N1—C1—C5—C6	-4.0 (5)	N4—N3—C5—C6	-2.7 (5)
C1—N1—C4—C3	0.1 (6)	N4—C7—C8—N5	-15.2 (4)
C1—C2—N2—C3	0.6 (6)	N4—C7—C8—C9	163.6 (3)
O2—N5—C8—C7	-179.9 (3)	C4—N1—C1—C2	-0.1 (6)
O2—N5—C8—C9	1.4 (5)	C4—N1—C1—C5	179.5 (3)
C2—C1—C5—N3	-5.8 (5)	C5—C1—C2—N2	-179.9 (3)
C2—C1—C5—C6	175.6 (4)	C5—N3—N4—C7	168.4 (3)
C2—N2—C3—C4	-0.5 (7)		

Hydrogen-bond geometry (\AA , $^\circ$)

<i>D</i> —H \cdots <i>A</i>	<i>D</i> —H	H \cdots <i>A</i>	<i>D</i> \cdots <i>A</i>	<i>D</i> —H \cdots <i>A</i>
O2—H2 \cdots O1 ⁱ	0.82	1.94	2.741 (3)	167
C2—H2 <i>A</i> \cdots O2 ⁱⁱ	0.93	2.35	3.243 (5)	161
C4—H4 <i>A</i> \cdots N2 ⁱⁱⁱ	0.93	2.67	3.451 (6)	142

Symmetry codes: (i) $-x+3/2, y+1, z+1/2$; (ii) $-x+3/2, y-1, z-1/2$; (iii) $-x+1, -y-1, z+1/2$.